LETTER

Onset of magnetic reconnection in a collisionless, high-β plasma

Andrew Alt[1,2] and Matthew W. Kunz[1,2,†]

[1]Department of Astrophysical Sciences, Princeton University, Peyton Hall, Princeton, NJ 08544, USA

[2]Princeton Plasma Physics Laboratory, PO Box 451, Princeton, NJ 08543, USA

In a magnetized, collisionless plasma, the magnetic moment of the constituent particles is an adiabatic invariant. An increase in the magnetic-field strength in such a plasma thus leads to an increase in the thermal pressure perpendicular to the field lines. Above a β-dependent threshold (where β is the ratio of thermal to magnetic pressure), this pressure anisotropy drives the mirror instability, producing strong distortions in the field lines on ion-Larmor scales. The impact of this instability on magnetic reconnection is investigated using a simple analytical model for the formation of a current sheet (CS) and the associated production of pressure anisotropy. The difficulty in maintaining an isotropic, Maxwellian particle distribution during the formation and subsequent thinning of a CS in a collisionless plasma, coupled with the low threshold for the mirror instability in a high-β plasma, imply that the geometry of reconnecting magnetic fields can differ radically from the standard Harris-sheet profile often used in simulations of collisionless reconnection. As a result, depending on the rate of CS formation and the initial CS thickness, tearing modes whose growth rates and wavenumbers are boosted by this difference may disrupt the mirror-infested CS before standard tearing modes can develop. A quantitative theory is developed to illustrate this process, which may find application in the tearing-mediated disruption of kinetic magnetorotational 'channel' modes.

Key words: astrophysical plasmas, plasma instabilities, plasma nonlinear phenomena

---

1. Introduction

Magnetic reconnection is the process by which magnetic energy is converted to plasma energy via a rapid topological rearrangement of magnetic-field lines (Zweibel & Yamada 2009; Yamada, Kulsrud & Ji 2010; Loureiro & Uzdensky 2016). It is usually preceded by a slow phase in which magnetic flux is accumulated in an increasingly thin current sheet (CS). Recently, it has been conjectured that this preparatory phase of CS formation, along with the material properties of the host plasma, determine the characteristics of the tearing modes that ultimately disrupt the sheet and thereby set the maximum aspect ratio above which CSs cannot survive

† Email address for correspondence: mkunz@princeton.edu

(Pucci & Velli 2014; Tenerani *et al.* 2015; Loureiro & Uzdensky 2016; Uzdensky & Loureiro 2016; Comisso *et al.* 2017; Huang, Comisso & Bhattacharjee 2017). This maximum aspect ratio is important for (at least) two reasons. First, the large aspect ratio of the Sweet–Parker CS (Parker 1957; Sweet 1958) in high-Lundquist-number plasmas, being violently unstable to the plasmoid instability (Loureiro, Schekochihin & Cowley 2007; Bhattacharjee *et al.* 2009), may not be realizable during CS formation. Second, the maximum aspect ratio may define a disruption scale in critically balanced Alfvénic turbulence, below which the intense, sheet-like structures become tearing unstable and break up (Boldyrev & Loureiro 2017; Loureiro & Boldyrev 2017*a*,*b*; Mallet, Schekochihin & Chandran 2017*a*,*b*).

All of the work thus far on CS formation and tearing-mediated disruption was either couched within a collisional magnetohydrodynamic (MHD) framework or focused on collisionless plasmas with $\beta \doteq 8\pi nT/B^2 \lesssim 1$ (n is the plasma density, T the temperature and B the magnetic-field strength). The latter restriction precludes application of those results to many dilute, weakly collisional astrophysical plasmas, whose large temperatures and relatively weak magnetic fields imply $\beta \gg 1$. For example, $n \sim 10^{-3}$ cm^{-3}, $T \sim 5$ keV and $B \sim 1$ µG in the hot intracluster medium (ICM) of galaxy clusters imply $\beta \sim 10^2$ (Carilli & Taylor 2002; Schekochihin & Cowley 2006); $n \sim 100$ cm^{-3}, $T \sim 2$ keV and $B \sim 1$ mG near the accretion radius of Sgr A* at the Galactic centre imply $\beta \sim 10$ (Quataert 2003; Marrone, Moran, Zhao & Rao 2007). The hallmark of such plasmas is that the embedded magnetic field, while energetically subdominant, nevertheless has a strength tens of orders of magnitude above that required to magnetize the plasma (i.e. $\Omega_i \tau \ggg 1$ and $\rho_i \lll L$, where $\Omega_i \doteq eB/m_i c$ is the ion-Larmor frequency, m_i is the ion mass, $\rho_i \doteq v_{\mathrm{th}i}/\Omega_i$ is the ion-Larmor radius, $v_{\mathrm{th}i} \doteq (2T/m_i)^{1/2}$ is the ion thermal speed and τ and L are representative macroscopic time and length scales, respectively). This hierarchy of scales, particularly in weakly collisional plasmas with collision frequencies ν satisfying $\nu\tau \ll 1$, biases the plasma properties with respect to the magnetic-field direction (Braginskii 1965). Notably, the thermal pressure becomes anisotropic.

There is a relatively large body of work on the impact of pressure anisotropy on tearing modes (Chen & Davidson 1981; Coppi 1983; Chen & Palmadesso 1984; Chen & Lee 1985; Ambrosiano, Lee & Fu 1986; Shi, Lee & Fu 1987; Karimabadi, Daughton & Quest 2005; Haijima *et al.* 2008; Quest, Karimabadi & Daughton 2010; Matteini *et al.* 2013; Gingell, Burgess & Matteini 2015), as well as on the production and impact of pressure anisotropy during the reconnection process itself (Drake *et al.* 2006; Le *et al.* 2009; Schoeffler, Drake & Swisdak 2011; Egedal, Le & Daughton 2013; Cassak *et al.* 2015; Le *et al.* 2016). Here we focus instead on the pressure anisotropy adiabatically produced during the CS formation, prior to the reconnection event. Namely, as the CS thins, the magnetic-field strength in the inflowing fluid elements increases. An increase in field strength in a weakly collisional, magnetized plasma leads, by adiabatic invariance, to an increase (decrease) in the thermal pressure perpendicular (parallel) to the field lines (Chew, Goldberger & Low 1956). Above an $O(1/\beta)$ threshold, this pressure anisotropy drives the mirror instability (Barnes 1966; Hasegawa 1969; Southwood & Kivelson 1993), which produces strong distortions in the field lines and traps particles on ion-Larmor scales (Kunz, Schekochihin & Stone 2014; Riquelme, Quataert & Verscharen 2015). In what follows, we ask how the production of pressure anisotropy during CS formation and the consequent triggering of ion-Larmor-scale mirror instabilities in a $\beta \gg 1$ plasma impacts the onset of tearing-mediated reconnection.

2. Prerequisites

2.1. *CS formation and pressure anisotropy*

We first establish that pressure anisotropy is produced during CS formation. For that, we adopt a simple local model for CS formation based on a one-dimensional generalization of the Chapman–Kendall solution (Chapman & Kendall 1963; Tolman, Loureiro & Uzdensky 2018, §2). A sheared magnetic field $\boldsymbol{B}(x,t) = B_\mathrm{r}[x/a(t)]\hat{\boldsymbol{y}} + B_\mathrm{g}\hat{\boldsymbol{z}}$ is frozen into an incompressible, time-independent fluid velocity $\boldsymbol{u}(x,y) = -(x\hat{\boldsymbol{x}} - y\hat{\boldsymbol{y}})/2\tau_\mathrm{cs}$, where B_r and $B_\mathrm{g} \doteq \theta B_\mathrm{r}$ are constants describing the strengths of the reconnecting and guide components of $\boldsymbol{B}$, respectively, and τ_cs is the characteristic CS-formation time scale. These expressions satisfy the reduced MHD equations provided that the CS half-thickness $a(t)$ and length $L(t)$ satisfy $a(t)/a_0 = L_0/L(t) = \exp(-t/\tau_\mathrm{cs})$, where the '0' subscript denotes an initial value. This model may be regarded as a Taylor expansion about the neutral line ($x = 0$) of a more complicated (e.g. Harris) CS profile, and so we restrict its validity to $|y| \ll L(t)$ and $|x| \lesssim a(t)$, beyond which $\boldsymbol{B}$ is taken to be spatio-temporally constant. (Indeed, this simple model is only meant to illustrate that $\Delta_p > 0$ can be driven during CS formation.) We assume $\sqrt{\rho_{i,\mathrm{r}}/a} \ll \theta \lesssim 1$ and $\Omega_i\tau_\mathrm{cs} \gg 1$, where $\rho_{i,\mathrm{r}}$ is the ion-Larmor radius computed using B_r, so that the entire CS is well magnetized (even near $x = 0$).[1]

Using these fields, it is straightforward to show that the magnetic-field strength in a fluid element starting at $x = \xi_0$ (with $|\xi_0| \leqslant a_0$) and moving towards $x = 0$ is

$$B(\xi(t), t) = B_\mathrm{r}[\theta^2 + \exp(t/\tau_\mathrm{cs})(\xi_0/a_0)^2]^{1/2}, \qquad (2.1)$$

where $\xi(t) = \xi_0 \exp(-t/2\tau_\mathrm{cs})$ is a Lagrangian coordinate co-moving with the fluid element. This change in B drives field-aligned pressure anisotropy, $\Delta_p \doteq p_\perp/p_\parallel - 1$, adiabatically in the fluid frame. Using μ conservation in the form $p_\perp \propto B$ and assuming $\Delta_p(x, t = 0) = 0$,

$$\Delta_p(\xi(t), t) = \left[\frac{\theta^2 + \exp(t/\tau_\mathrm{cs})(\xi_0/a_0)^2}{\theta^2 + (\xi_0/a_0)^2}\right]^{1/2} - 1 \approx \frac{t}{2\tau_\mathrm{cs}}\frac{(\xi_0/a_0)^2}{\theta^2 + (\xi_0/a_0)^2} \doteq \frac{t}{\tau_\mathrm{pa}} \qquad (2.2)$$

for $t/\tau_\mathrm{cs} \ll 1$.[2] Thus, pressure anisotropy increases in all fluid elements.

If nothing interferes with the adiabatic increase in pressure anisotropy, the plasma in a fluid element will eventually become mirror unstable when $\Delta_p \gtrsim 1/\beta_\perp$, where

$$\beta_\perp(\xi(t), t) = \beta_0(\xi_0) \left[\frac{\theta^2 + (\xi_0/a_0)^2}{\theta^2 + \exp(t/\tau_\mathrm{cs})(\xi_0/a_0)^2}\right]^{1/2} \approx \beta_0 \left(1 - \frac{t}{3\tau_\mathrm{pa}}\right) \qquad (2.3)$$

is the adiabatically evolving perpendicular plasma β in the fluid frame (β_0 is its initial value). Comparing (2.2) and (2.3), this occurs at $t_\mathrm{m} \sim \tau_\mathrm{pa}/\beta_0$ for $\beta_0 \gg 1$. If the guide field is small compared to the local reconnecting field ($\theta \ll \xi_0/a_0$), this time is a small fraction of the CS-formation time scale, $t_\mathrm{m} \sim \tau_\mathrm{cs}/\beta_0$, and so the CS becomes mirror unstable early in its evolution. With a larger guide field ($\theta \gg \xi_0/a_0$), $t_\mathrm{m} \sim \tau_\mathrm{cs}(a_0^2/\xi_0^2)(\theta^2/\beta_0)$. This time is also early in the CS evolution for $\xi_0 \lesssim a_0$,

---

[1]This guarantees that any particle whose guiding centre lies near $x = 0$ executes Larmor motion about B_g rather than a betatron orbit with turning points at $\sim\sqrt{\rho_{i,\mathrm{r}}a}$ (as in Dobrowolny 1968).

[2]If the second adiabatic invariant, J, were also conserved – unlikely in a $\beta \gg 1$ plasma with Alfvénic, incompressible flows – the exponent $1/2$ in (2.2) becomes $3/2$ and τ_pa changes by an inconsequential factor of 3.

since $\theta \ll \beta^{1/2}$ is required in this model for the plasma to reliably exceed the mirror-instability threshold.[3]

These times must be compared to the characteristic time scales for tearing modes that facilitate magnetic reconnection in the forming CS. Before doing so, we review the basic properties of the mirror instability.

2.2. *Mirror instability*

As B increases, adiabatic invariance drives $\Delta_p > 0$, with plasma becoming mirror unstable when $\Lambda_m \doteq \Delta_p - 1/\beta_\perp > 0$. Just beyond this threshold ($0 < \Lambda_m \ll 1$), oblique modes with wavenumbers $k_{\parallel,m}\rho_i \sim (k_{\perp,m}\rho_i)^2 \sim \Lambda_m$ and polarization $\delta B_\perp/\delta B_\parallel \sim \Lambda_m^{1/2}$ grow exponentially at a maximum rate $\gamma_m \sim \Omega_i \Lambda_m^2$ (Hellinger 2007). Once this growth rate becomes larger than the rate at which Δ_p is produced ($\gamma_m \tau_{pa} \gtrsim 1$), the growth of Δ_p stops. This yields a maximum mirror-instability parameter, $\Lambda_m \gtrsim (\Omega_i \tau_{pa})^{-1/2} \doteq \Lambda_{m,max}$. Kinetic simulations show that, once $\Lambda_m(t) \sim \Lambda_{m,max}$, mirrors rapidly drain $\Lambda_m(t) \to 0^+$ and attain amplitudes $\delta B_\parallel/B \sim \Lambda_{m,max}^{1/2}$ (Kunz *et al.* 2014). This is the end of the linear stage; for $\beta_0 \gg 1$, this occurs at $t/\tau_{pa} \sim 1/\beta_0 + \Lambda_{m,max}$.

As the CS continues to thin, $\Delta_p > 0$ is continuously driven. Mirror modes then maintain marginal stability ($\Lambda_m \simeq 0^+$) by growing secularly, $\delta B_\parallel^2 \propto t^{4/3}$, and trapping an increasing fraction of particles (Schekochihin *et al.* 2008; Kunz *et al.* 2014; Rincon, Schekochihin & Cowley 2015). Independent of $\Lambda_{m,max}$, saturation occurs at $t \sim \tau_{pa}$ and $\delta B/B \sim 1$, when these particles pitch-angle scatter off sharp bends in the magnetic field occurring at the mirror boundaries at a rate $\nu_m \sim \beta/\tau_{pa}$; this maintains marginal stability by severing the adiabatic link between Δ_p and changes in B (Kunz *et al.* 2014; Riquelme *et al.* 2015). Thereafter, $\Delta_p \simeq 1/\beta_\perp$, even as B changes.

This evolution was found for situations in which τ_{pa} is comparable to the dynamical time in the system (e.g. linear shear flows). However, for locations $\xi_0 \ll \theta a_0$ deep inside the CS, $\tau_{pa} \gg \tau_{cs}$. In this case, local mirror growth cannot outpace CS formation, and any potential mirrors are advected and distorted faster than they can grow. When $\theta \gg 1$, $\tau_{pa} \gg \tau_{cs}$ in the entire CS. We thus focus only on cases with $\theta \lesssim 1$ and locations $\xi_0 \gtrsim \theta a_0$.

2.3. *Collisionless tearing instability*

Next we review the theory of collisionless tearing modes, applicable when the inner-layer thickness of the tearing CS, $\delta_{in} \lesssim \rho_e$. To determine under what condition this criterion is satisfied, we use standard MHD tearing theory (Furth, Killeen & Rosenbluth 1963; FKR) to estimate

$$\delta_{in}^{MHD} = [\gamma_t (k_t v_{A,r})^{-2} a^2 \eta]^{1/4} = a[\gamma_t \tau_{A,r} (k_t a)^{-2} S_a^{-1}]^{1/4}, \qquad (2.4)$$

where $v_{A,r} \doteq B_r/(4\pi m_i n_i)^{1/2}$ is the Alfvén speed of the reconnecting field, $\tau_{A,r} \doteq a/v_{A,r}$ is the Alfvén crossing time of the CS, η is the (collisional) resistivity and $S_a \doteq a v_{A,r}/\eta$ is the Lundquist number. Using an estimate for the growth rate γ_t of the fastest-growing collisional tearing mode with wavenumber k_t oriented along the CS (Furth *et al.* 1963; Coppi *et al.* 1976; Uzdensky & Loureiro 2016), the validity condition for collisionless tearing theory to hold becomes

$$S_a \gtrsim (a/\rho_e)^4. \qquad (2.5)$$

---

[3] If the asymptotic value of the reconnecting field, B_r, is constant, then the maximum change of B in a fluid element is bounded, $B(t)/B(0) < (1 + \theta^{-2})^{1/2}$, and so $\Delta_p < (1 + \theta^{-2})^{1/2} - 1$. Therefore, $\theta \lesssim \beta^{1/2}$ is required to reach the mirror threshold. In other models where B_r increases in time (e.g. Tolman *et al.* 2018), no such limit on θ exists.

This gives $a \lesssim 10^{-6}$ pc for the ICM parameters listed in §1, a satisfiable constraint given that $\rho_i \sim 10^{-9}$ pc and the outer scale of ICM magnetic-field fluctuations is observationally inferred to be ~ 10 kpc (Enßlin & Vogt 2006; Guidetti *et al.* 2008; Bonafede *et al.* 2010; Vacca *et al.* 2012; Govoni *et al.* 2017), comparable to the collisional mean free path. At the accretion radius of Sgr A*, this constraint is $a \lesssim 10^{-10}$ pc, which is $\sim 10^2$ larger than ρ_i and $\sim 10^8$ times smaller than the collisional mean free path. As long as (2.5) is satisfied (which becomes easier as a shrinks), γ_t and k_t are estimated as follows.

In a $\beta \gtrsim 1$ plasma when the tearing-mode instability parameter $\Delta'(k_t)$ (Furth *et al.* 1963) is small, satisfying $\Delta' \delta_{in} \sim (\Delta' d_e)^2 \ll 1$ ('FKR-like'; Karimabadi *et al.* (2005)),

$$\gamma_t^{\text{FKR}} \tau_{\text{A,r}} \sim \left(\frac{m_e}{m_i}\right)^{1/2} \left(\frac{d_i}{a}\right)^2 k_t a \Delta' a, \tag{2.6}$$

where d_e and $d_i \doteq \rho_i / \beta_i^{1/2} = d_e (m_i/m_e)^{1/2}$ are, respectively, the electron and ion skin depths (Fitzpatrick & Porcelli 2004, 2007). (Our CS formation model leaves d_e, d_i constant.) This growth rate is approximately independent of k_t in a Harris sheet, for which $\Delta' a = 2(1/k_t a - k_t a) \sim (k_t a)^{-1}$ at $k_t a \ll 1$. The large-Δ' ('Coppi-like') growth rate satisfies

$$\gamma_t^{\text{Coppi}} \tau_{\text{A,r}} \sim \left(\frac{m_e}{m_i}\right)^{1/5} \left(\frac{d_i}{a}\right) k_t a, \tag{2.7}$$

independent of Δ' (Fitzpatrick & Porcelli 2007). An estimate for γ_t and k_t of the fastest-growing Coppi-like mode in a Harris sheet can be obtained by balancing (2.6) and (2.7):

$$\gamma_t^{\text{max}} \tau_{\text{A,r}} \sim \left(\frac{m_e}{m_i}\right)^{1/2} \left(\frac{d_i}{a}\right)^2, \tag{2.8a}$$

$$k_t^{\text{max}} a \sim \left(\frac{m_e}{m_i}\right)^{3/10} \left(\frac{d_i}{a}\right). \tag{2.8b}$$

These modes are the fastest growing provided they fit into the length L of the CS, i.e. $k_t^{\text{max}} L > 1$. Otherwise, the fastest-growing mode is FKR-like.[4]

In what follows, we assume that pressure anisotropy does not appreciably modify these growth rates. This is because saturated mirrors maintain $\Delta_p \simeq 1/\beta_\perp \ll 1$, and so the resulting viscous stress effectively enhances the magnetic tension responsible for driving the tearing by a factor of only $\simeq 3/2$. Other works that postulate an initial Δ_p (customarily taken to be uniform and thus non-zero even at $x = 0$) do not consider its rapid regulation by the mirror instability prior to the onset of tearing, and the

---

[4]Fitzpatrick & Porcelli (2004, 2007) obtained (2.6) and (2.7) using a two-fluid model assuming cold ions and that the compressional Alfvén wave propagates much faster than any other wave in the system (as it would in a high-β plasma), thus guaranteeing pressure balance along field lines and nearly incompressible flow. The former (small-Δ') growth rate agrees with the corresponding kinetic expression in Drake & Lee (1977*a*, their equation (16)) up to a factor of $1/\sqrt{1 + \beta_g}$, which is ~ 1 given those authors' assumption of small β and large guide field. Both results assumed a Maxwellian background. Alternatively, Chen & Palmadesso (1984) allowed for a spatially uniform $\Delta_p \neq 0$ in their linear kinetic tearing calculation, but assumed $B_g = 0$ and thus obtained different scalings after accounting for axis-crossing particle orbits (see also Chen & Lee (1985) and Quest *et al.* (2010)). While we have opted to use the Fitzpatrick & Porcelli (2004, 2007) expressions for γ_t, our analysis can be generalized for any alternative scalings without a significant change in the main qualitative conclusions summarized in §5. The 'FKR-like' and 'Coppi-like' designations are adaptations of those introduced by Uzdensky & Loureiro (2016).
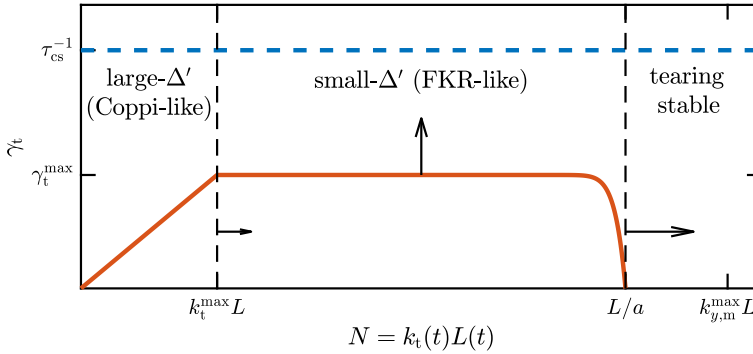
FIGURE 1. Qualitative plot of tearing growth rate γ_t versus mode number N (see (2.6) and (2.7)) shortly after mirror production at $k_{y,m}^{max} a > 1$. Arrows indicate evolution as the CS aspect ratio (L/a) increases, with γ_t approaching τ_{cs}^{-1} (blue dashed line), k_t approaching the large-Δ' regime ($k_t \lesssim k_t^{max}$) and mirrors affecting an increasing number of tearing modes (those with $k_t \gtrsim k_{y,m}^{max}$).

enhanced γ_t often found in linear calculations when $\Delta_p > 0$ is largely because the assumption $B_g = 0$ permits axis-crossing particle orbits in the inner regions of the CS and allows threshold-less instabilities such as the Weibel instability (e.g. Chen & Palmadesso 1984).

3. Reconnection onset when $\Delta_p = 0$

Before determining how mirror-unstable pressure anisotropy affects a gradually forming CS, we recapitulate the theory of CS disruption by tearing modes (Pucci & Velli 2014; Tenerani *et al.* 2015; Loureiro & Uzdensky 2016; Uzdensky & Loureiro 2016), specialized to the case of collisionless tearing in a high-β plasma. That is, we ignore the production of pressure anisotropy during CS formation and instead determine when L/a has increased enough for tearing modes to prompt reconnection.

As the CS's aspect ratio L/a increases in time, modes with progressively larger mode number $N \doteq k_t(t)L(t) = $ const. become unstable and undergo linear evolution with $\gamma_t(N,t)$ increasing (see figure 1). Uzdensky & Loureiro (2016) argued that the first tearing mode N to reach the end of its linear stage at the critical time $t_{cr}(N)$ (when $\gamma_t \tau_{cs} \gtrsim 1$, neglecting logarithmic corrections (Comisso *et al.* 2017)) will also be the first to undergo X-point collapse (defined by when the island width $w \sim 1/\Delta'$) and, soon thereafter, disrupt the CS ($w \sim a$). We adopt this argument and estimate the CS disruption time $t_{disrupt}$ for a collisionless Harris sheet with $L(t)a(t) = $ const. (The same procedure can be used to investigate alternative CS profiles and evolution.) Note that, for the Harris-sheet profile, $\gamma_t^{FKR} \approx \gamma_t^{max}$ for $k_t a \ll 1$ (see (2.6) and (2.8a)), so the only difference between these modes are their wavenumbers and, thus, their $\Delta' \sim 1/k_t a^2$.

Each unstable mode N starts in the small-Δ' ('FKR-like') regime ($N > N_{max}(t)$), with γ_t roughly independent of k_t for $k_t a \ll 1$. However, because $N_{max} \propto (L/a)(d_i/a) \propto a^{-3}$ increases in time, these FKR-like modes approach the large-Δ' ('Coppi-like') regime, making the transition at $t = t_{tr}(N)$ when

$$\frac{a(t_{tr}(N))}{a_0} \sim \left(\frac{m_e}{m_i}\right)^{1/10} \left(\frac{L_0 d_i}{a_0^2}\right)^{1/3} N^{-1/3}. \qquad (3.1)$$

Larger N corresponds to larger $t_{\mathrm{tr}}(N)$, and so the first mode to make this transition is $N = 1$; i.e. at $t = t_{\mathrm{tr}}(1)$, the fastest Coppi-like mode (see (2.8b)) just fits inside the CS. All modes satisfying $k_{\mathrm{t}}^{\max} a \lesssim k_{\mathrm{t}} a \ll 1$ obtain growth rates $\gamma_{\mathrm{t}} \tau_{\mathrm{cs}} \gtrsim 1$ at roughly the same time, $t = t_{\mathrm{cr}}$, when (using (2.8a))

$$\frac{a(t_{\mathrm{cr}})}{a_0} \lesssim \left(\frac{m_e}{m_i}\right)^{1/6} \left(\frac{d_i}{a_0}\right)^{2/3} M_{\mathrm{A},0}^{-1/3}, \tag{3.2}$$

where $M_{\mathrm{A},0} \doteq \tau_{\mathrm{A,r}}(t=0)/\tau_{\mathrm{cs}}$ is the initial Alfvénic Mach number of the CS formation. These modes have

$$\frac{L(t_{\mathrm{cr}})}{a(t_{\mathrm{cr}})} \gg N \geqslant N_{\mathrm{cr}} \doteq \left(\frac{m_e}{m_i}\right)^{-1/5} \left(\frac{L_0}{d_i}\right) M_{\mathrm{A},0}. \tag{3.3}$$

This is an important distinction from the collisional MHD case, in which larger $N > N_{\mathrm{cr}}$ corresponds to larger $t_{\mathrm{cr}}(N)$ (since $\gamma_{\mathrm{t}}^{\mathrm{FKR}} \propto k_{\mathrm{t}}^{-2/5}$ at $k_{\mathrm{t}} a \ll 1$ instead of k_{t}^0).

Another important distinction from the MHD case lies in the nonlinear evolution, during which the MHD FKR modes behave differently than the MHD Coppi modes. While the latter are expected to rapidly evolve towards X-point collapse soon after $t = t_{\mathrm{cr}}$ due to their large Δ', the former undergo secular 'Rutherford' evolution that increases $\Delta'(k_N) w_N$ for a given mode N until $w_N \sim 1/\Delta'$ (Rutherford 1973; Waelbroeck 1989, 1993; Loureiro *et al.* 2005; Arcis, Loureiro & Militello 2009). However, in the collisionless case, the FKR-like modes reach $\gamma_{\mathrm{t}} \tau_{\mathrm{cs}} \sim 1$ at the same time as the fastest Coppi-like mode. If the latter is accessible, then the fastest-growing mode $N_{\max}$ already has $\Delta' d_e \sim 1$ at $t_{\mathrm{cr}}(N_{\max})$ and so X-point collapse likely occurs soon after (3.2) is satisfied. The CS is then said to be 'disrupted' at $t_{\mathrm{disrupt}} \sim t_{\mathrm{cr}}(N_{\max})$. For there to be no Coppi-like modes when (3.2) is satisfied (i.e. $N_{\mathrm{cr}} < 1$), $M_{\mathrm{A},0} \lesssim (m_e/m_i)^{1/5}(d_i/L_0)$, a rather stringent condition that is difficult to satisfy when $\beta_0 \gg 1$ and $\rho_{i0}/L_0 \ll 1$.

That being said, given the uncertainties in the nonlinear evolution of collisionless tearing modes in a high-β, magnetized plasma – especially regarding the existence (or non-existence) of a secular 'Rutherford' phase and the production of pressure anisotropy during X-point collapse – we focus primarily on the critical time for reconnection onset (when $\gamma_{\mathrm{t}} \tau_{\mathrm{cs}} \gtrsim 1$) rather than the CS disruption time (when $w \sim a$).[5]

4. Reconnection onset when $\Delta_p \neq 0$

We now consider the effects of mirrors on an evolving CS subject to tearing modes. Because different portions of the CS have different ρ_i and τ_{pa}, there will be a range of mirror wavenumbers, $k_{y,\mathrm{m}}(x)$, along the CS (see figure 2).

The smallest $k_{y,\mathrm{m}}$ will be located the nearest to $x = 0$ where mirrors can form, since these regions have the largest values of ρ_i and τ_{pa}. We argue that, since tearing modes with wavenumbers k_{t} much smaller than this $k_{y,\mathrm{m}}^{\min}$ will see a rapidly y-varying magnetic field that averages to its unperturbed value, these modes are likely unaffected by the mirrors (or at least less affected than other modes). The largest $k_{y,\mathrm{m}}$ will be located near $|x| \sim a$, where ρ_i and τ_{pa} are at their smallest values. All tearing modes with $k_{\mathrm{t}} \gg k_{y,\mathrm{m}}^{\max}$ will see an approximately uniform-in-y magnetic field, but will have their

---

[5]Another reason for prudence is Drake & Lee's (1977b) argument that single-mode tearing with a guide field saturates via trapped-electron effects with an amplitude comparable to the inner-layer thickness, $w \sim \delta_{\mathrm{in}}$. This argument was confirmed, and refined by incorporating finite-Larmor-radius effects, by Karimabadi *et al.* (2005).
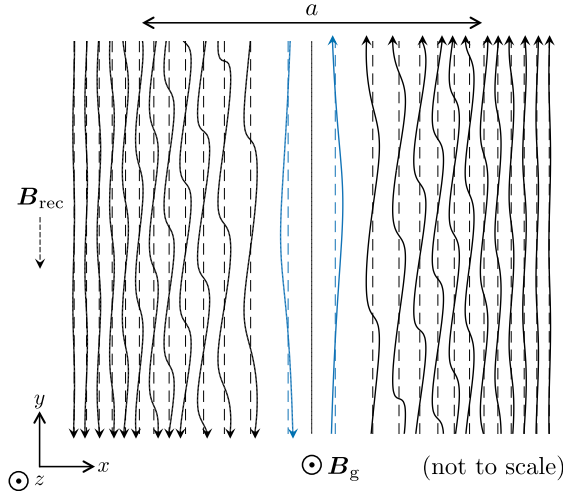
FIGURE 2. Qualitative illustration of magnetic-field lines in an evolving, mirror-infested Harris CS with $\theta \ll 1$.

$\Delta'(k_t)$ enhanced by the mirrors' effect on the x-variation of the CS profile. If the CS is able to stretch to the point where $k_{y,\mathrm{m}}^{\max} \lesssim k_t^{\max}$ before the onset of tearing, then all of the modes that are unaffected by the mirrors will have smaller growth rates and thus be unimportant for CS reconnection. The condition $k_{y,\mathrm{m}}^{\max} \lesssim k_t^{\max}$ is thus a sufficient (but not necessary) condition for mirrors to matter.

We now follow the evolution of $k_{y,\mathrm{m}}^{\max}$ as the CS evolves, and investigate the evolution of tearing modes with $k_t \gg k_{y,\mathrm{m}}^{\max}$. We treat two cases, depending upon the size of the guide field and thus the component of the mirrors' wavevector along the CS at $|x| \sim a$,

$$k_{y,\mathrm{m}} \sim k_{\parallel,\mathrm{m}} \frac{B_r}{B} + k_{\perp,\mathrm{m}} \frac{B_g}{B} = k_{\parallel,\mathrm{m}} \frac{B_r}{B} \left(1 + \theta \frac{k_{\perp,\mathrm{m}}}{k_{\parallel,\mathrm{m}}}\right). \tag{4.1}$$

With $k_{\perp,\mathrm{m}}/k_{\parallel,\mathrm{m}} \sim \Lambda_{\mathrm{m,max}}^{-1/2}$ for the fastest-growing mirror mode, we have $k_{y,\mathrm{m}} \sim k_{\parallel,\mathrm{m}}$ for $\theta \ll \Lambda_{\mathrm{m,max}}^{1/2}$ and $k_{y,\mathrm{m}} \sim \theta k_{\perp,\mathrm{m}}$ for $\Lambda_{\mathrm{m,max}}^{1/2} \ll \theta \lesssim 1$. (In both cases, $\Lambda_{\mathrm{m,max}} \sim (d_i/a_0)^{1/2} M_{\mathrm{A},0}^{1/2}$.)

4.1. *When mirrors affect tearing if* $\theta \ll \Lambda_{\mathrm{m,max}}^{1/2}$

At $x \sim a$, the local reconnecting field is near its asymptotic value and $\tau_{\mathrm{pa}} \sim \tau_{\mathrm{cs}}$. Starting at time $t_{\mathrm{m}} \sim \tau_{\mathrm{cs}}/\beta_0 \ll \tau_{\mathrm{cs}}$, unstable mirror modes grow rapidly at this location (a and $\tau_{\mathrm{A,r}}$ hardly change from their initial values in a time t_{m}.) Unless tearing modes disrupt the CS within $t_{\mathrm{disrupt}} \lesssim \tau_{\mathrm{cs}}$ – which is extremely unlikely, requiring (3.2) to be satisfied within τ_{cs} – these mirrors will saturate with $\delta B \sim B_r$ and

$$k_{y,\mathrm{m}}^{\max}(t)\rho_i \sim \frac{L_0}{L(t)}(\Omega_i \tau_{\mathrm{cs}})^{-1/2} \sim \frac{a(t)}{a_0}\left(\frac{d_i}{a_0}\right)^{1/2} M_{\mathrm{A},0}^{1/2}, \tag{4.2}$$

where we have accounted for the Lagrangian stretching of the perturbations during CS formation.

To determine the effect of these mirrors on tearing, it is useful (as argued above) to first establish when $k_{y,\mathrm{m}}^{\max}(t)$ enters the large-Δ' regime in which $\gamma_{\mathrm{t}} \propto k$ (the leftmost portion of figure 1), i.e. when the mirrors influence the fastest-growing tearing modes. Combining (2.8b) and (4.2), we find that $a(t)$ must satisfy

$$\frac{a(t)}{d_i} \lesssim \left(\frac{m_e}{m_i}\right)^{1/10} \left(\frac{d_i}{a_0}\right)^{-1/2} \beta_0^{1/6} M_{\mathrm{A},0}^{-1/6} \tag{4.3}$$

for $k_{y,\mathrm{m}}^{\max}(t) \lesssim k_{\mathrm{t}}^{\max}(t)$. Equation (4.3) happens before the sheet would be disrupted in the absence of mirrors (see (3.2)) if

$$\frac{a_0}{d_i} \gtrsim \left(\frac{m_e}{m_i}\right)^{2/5} \beta_0^{-1} M_{\mathrm{A},0}^{-1}, \tag{4.4}$$

which is easily satisfied under the conditions of interest. Thus, there will be a time at which all tearing modes with $k_{\mathrm{t}} \gtrsim k_{\mathrm{t}}^{\max}$ are affected by mirrors. How the tearing progresses after (4.3) is satisfied will be discussed once the corresponding conditions for the other θ-regime are derived.

4.2. *When mirrors affect tearing if $\Lambda_{\mathrm{m,max}}^{1/2} \ll \theta \lesssim 1$*

As B_{g} is increased, things will continue in much the same way as in § 4.1 except that the initial $k_{y,\mathrm{m}}^{\max} \sim \theta k_{\perp,\mathrm{m}}$. That is, equation (4.2) is replaced by

$$k_{y,\mathrm{m}}^{\max}(t)\rho_i \sim \frac{L_0}{L(t)} \theta (\Omega_i \tau_{\mathrm{cs}})^{-1/4} \sim \frac{a(t)}{a_0} \left(\frac{d_i}{a_0}\right)^{1/4} \theta M_{\mathrm{A},0}^{1/4}. \tag{4.5}$$

This means that the condition on $a(t)$ that $k_{y,\mathrm{m}}^{\max}(t) \lesssim k_{\mathrm{t}}^{\max}(t)$ (cf. (4.3)) becomes

$$\frac{a(t)}{d_i} \lesssim \left(\frac{m_e}{m_i}\right)^{1/10} \left(\frac{d_i}{a_0}\right)^{-5/12} \theta^{-1/3} \beta_0^{1/6} M_{\mathrm{A},0}^{-1/12}. \tag{4.6}$$

If the initial state satisfies

$$\frac{a_0}{d_i} \gtrsim \left(\frac{m_e}{m_i}\right)^{4/5} \theta^4 \beta_0^{-2} M_{\mathrm{A},0}^{-3}, \tag{4.7}$$

then (4.6) occurs before (3.2), when the sheet would be disrupted without the mirrors.

4.3. *Mirror-stimulated onset of reconnection*

If either (4.4) or (4.7) is satisfied, then mirrors influence all tearing modes before they could otherwise disrupt the CS in the absence of mirrors. We now quantify that influence, focusing on those tearing modes with $k_{\mathrm{t}} \gg k_{y,\mathrm{m}}^{\max}$ (see (4.2) and (4.5)). As argued previously, these modes see a magnetic field that is roughly uniform in y but is rapidly varying in x due to the mirrors, with an initial $k_{x,\mathrm{m}} \sim k_{\perp,\mathrm{m}}$ that is then compressed by the CS formation with $k_{x,\mathrm{m}}(t)a(t) \sim \mathrm{const}$. This rapid variation enhances $\gamma_{\mathrm{t}}(k_{\mathrm{t}})$ for these modes due to the smaller effective sheet thickness (estimated below), which affects both $\Delta'(k_{\mathrm{t}})$ and the Alfvén-crossing time $\tau_{\mathrm{A,r}}$ (see (2.6) and (2.7)).

4.3.1. *Model for a mirror-infested CS*

We argue that $\tau_{A,r}$ changes by a small amount, since mirrors modify $dB_y/dx|_{x=0}$ by only a factor of order unity. To determine how $\Delta'(k)$ is modified, we adopt the following simple model for the magnetic-field profile of a mirror-infested Harris CS:

$$B_y(x) = B_r \tanh\left(\frac{x}{a}\right)\left[1 + \varepsilon \sin\left(2k_{\max}a\,\mathrm{sech}\left(\frac{x}{a}\right)\right)\right], \quad (4.8)$$

where $k_{\max} \gg a^{-1}$ is a parameter characterizing the peak $k_{x,m}$ occurring at the edge of the CS. This is a Wentzel–Kramers–Brillouin (WKB) approximation describing saturated mirrors with amplitude $\varepsilon \sim O(1)$ times the local reconnecting field and wavenumber in the x-direction given by $k_x(x) = 2k_{\max}\,\mathrm{sech}(x/a)\tanh(x/a)$. This model was chosen because $k_x(x=0) = 0$, $k_x(x \to \infty) \to 0$, and $k_x(x)$ is maximal near the edge of the CS, as anticipated. (What follows is not particularly sensitive to this choice of $k_x(x)$.)

The resulting $\Delta'(k_t)$ is obtained by numerically integrating the outer differential equation for the flux function, ψ (Furth *et al.* 1963):

$$\frac{d^2\psi}{dx^2} - \left(k^2 + \frac{B_y''}{B_y}\right)\psi = 0, \quad (4.9)$$

with $B_y(x)$ given by (4.8). Then $\Delta' \doteq d\ln\psi/dx|_{x=0}$ for the solution that obeys reasonable boundary conditions; an example result is shown in figure 3(*a*). (Its shape does not change significantly as ε and $k_{\max}$ vary.) Generally, $\Delta' > 0$ for k_t smaller than the inverse of the effective sheet thickness, a_{eff}, which we identify with the location x_m of the peak in $B_y(x)$ closest to $x = 0$ (i.e. the location of the innermost mirror). As k_t decreases from this value, $\Delta'(k_t)$ rises sharply to saturate at $k_t = k_{\mathrm{sat}}$ with value $\Delta'_{\mathrm{sat}} \sim 1/a_{\mathrm{eff}} \sim 1/x_m$, at which it is approximately constant until it nears the Harris-sheet $\Delta'(k_t) \sim 1/k_t a^2$, which it then follows.

The corresponding $\gamma_t(k_t)$ shown in figure 3(*b*) depends on whether or not $\Delta'_{\mathrm{sat}}d_e \ll 1$. However, the maximum growth rate always occurs at $k_{\mathrm{sat}} \sim 1/x_m$, because of the k_t-dependence of (2.6) and (2.7). Thus, to determine the new t_{cr}, we must calculate x_m. This yields two cases based on the size of θ.

4.3.2. *Mirror-stimulated tearing for $\theta \ll x_m/a$*

When the reconnecting field is the dominant field on the scale of the innermost mirrors, the total ion-Larmor frequency is $\Omega_i \sim (x_m/a)\Omega_{i,r}$ and $\tau_{pa} \sim \tau_{cs}$. The x-wavenumber of the mirrors at that location is then

$$k_{x,m}(t, x_m(t))\rho_{i,r} \sim \left(\frac{x_m}{a(t)}\right)^{3/4}\left(\frac{d_i}{a_0}\right)^{1/4}\frac{a_0}{a(t)}M_{A,0}^{1/4}, \quad (4.10)$$

where we have accounted for the Lagrangian compression due to CS formation. The innermost mirror is located at $x_m \sim k_{x,m}^{-1}$, an x-wavelength away from the centre. Substituting this into (4.10) yields

$$\frac{x_m}{a(t)} \sim \left(\frac{d_i}{a_0}\right)^{3/7}\beta_r^{2/7}M_{A,0}^{-1/7}. \quad (4.11)$$

For this estimate to be self-consistent, we require $\theta \ll x_m/a$ or, using (4.11),

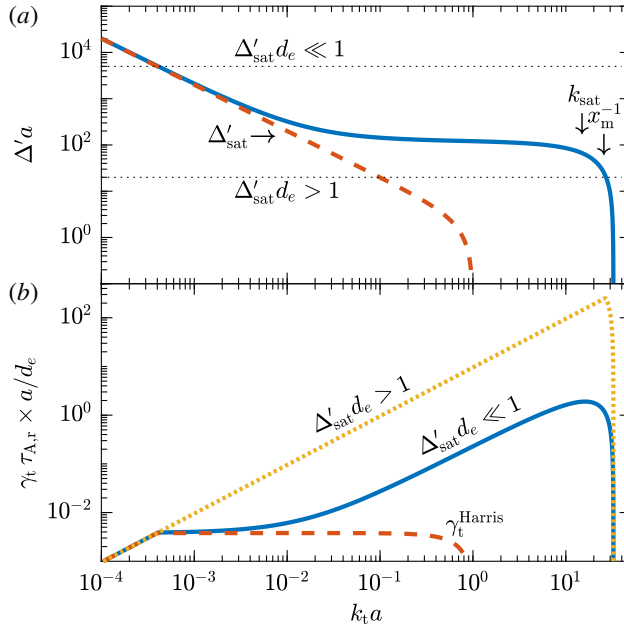$$\theta \ll \left(\frac{d_i}{a_0}\right)^{3/7}\beta_r^{2/7}M_{A,0}^{-1/7}. \quad (4.12)$$

FIGURE 3. Values of (*a*) $\Delta'(k_t)$ and (*b*) $\gamma_t(k_t)$ for a Harris CS (red dashed line) and its mirror-infested counterpart (blue solid line), using $k_{\max}a = 200\pi$ and $\varepsilon = 1/2$ in (4.8): Δ' rises rapidly at $k_t x_m \lesssim 1$ and plateaus for $k_{\text{sat}} \gtrsim k_t \gtrsim 1/(\Delta'_{\text{sat}}a^2)$. Mirror-stimulated tearing thus peaks at $k_t \sim k_{\text{sat}}$, regardless of whether $\Delta'_{\text{sat}}d_e \ll 1$ (blue solid line) or $\Delta'_{\text{sat}}d_e \gtrsim 1$ (orange dotted line).

Provided this is satisfied, the fastest-growing tearing mode, having $\gamma_t(k_{\text{sat}})$, is either FKR-like, if $d_e/x_m \ll 1$, or Coppi-like, if $d_e/x_m \gtrsim 1$.

In the former case, the maximum tearing growth rate is (using (2.6) with $k_t \sim 1/x_m$ and $\Delta' \sim 1/x_m$)

$$\gamma_{t,m}^{\text{FKR}}\tau_{A,r} \sim \left(\frac{m_e}{m_i}\right)^{1/2} \left(\frac{d_i^{8/7} a_0^{6/7}}{a^2}\right) \beta_r^{-4/7} M_{A,0}^{2/7}. \tag{4.13}$$

The critical time for onset, $t_{\text{cr}}^{\text{FKR}}$, occurs when $\gamma_{t,m}^{\text{FKR}}\tau_{\text{cs}} \sim 1$, or

$$\frac{a(t_{\text{cr}}^{\text{FKR}})}{a_0} \lesssim \left(\frac{m_e}{m_i}\right)^{1/6} \left(\frac{d_i}{a_0}\right)^{8/21} \beta_r^{-4/7} M_{A,0}^{-5/21}. \tag{4.14}$$

In the latter (Coppi-like) case, which happens when

$$\frac{a(t_{\text{tr}})}{a_0} \lesssim \left(\frac{m_e}{m_i}\right)^{1/2} \left(\frac{d_i}{a_0}\right)^{4/7} \beta_r^{-2/7} M_{A,0}^{1/7}, \tag{4.15}$$

the maximum growth rate is

$$\gamma_{t,m}^{\text{Coppi}}\tau_{A,r} \sim \left(\frac{m_e}{m_i}\right)^{1/5} \beta_r^{-2/7} M_{A,0}^{1/7} \left(\frac{d_i^{4/7} a_0^{3/7}}{a}\right), \tag{4.16}$$

and so the critical time $t_{\mathrm{cr}}^{\mathrm{Coppi}}$ occurs when $\gamma_{\mathrm{t,m}}^{\mathrm{Coppi}} \tau_{\mathrm{cs}} \sim 1$, or

$$\frac{a(t_{\mathrm{cr}}^{\mathrm{Coppi}})}{a_0} \lesssim \left(\frac{m_e}{m_i}\right)^{1/10} \left(\frac{d_i}{a_0}\right)^{2/7} \beta_{\mathrm{r}}^{-1/7} M_{\mathrm{A,0}}^{-3/7}. \tag{4.17}$$

If the smallest parameter in the problem is d_i/a_0, so that (4.14) occurs before (4.15) (i.e. $t_{\mathrm{cr}}^{\mathrm{FKR}} < t_{\mathrm{tr}}$), then the CS will go unstable to mirror-stimulated FKR-like modes before the fastest-growing mode enters the large-Δ' regime. In this case, the critical CS thickness, a_{cr}, is given by (4.14). Comparing this to the expression for a_{cr} when pressure anisotropy is not considered, equation (3.2), we see that mirrors increase a_{cr} by a factor of $\sim (d_i/a_0)^{-2/7} \beta_{\mathrm{r}}^{-4/7} M_{\mathrm{A,0}}^{2/21}$. If, instead, $t_{\mathrm{cr}}^{\mathrm{FKR}} > t_{\mathrm{tr}}$, then the fastest-growing mirror-stimulated tearing mode becomes Coppi-like before tearing onsets, and a_{cr} is effectively increased by a factor of $\sim (m_e/m_i)^{-1/15} (d_i/a_0)^{-8/21} \beta_{\mathrm{r}}^{-1/7} M_{\mathrm{A,0}}^{-2/21}$.

4.3.3. *Mirror-stimulated tearing for* $\theta \sim x_{\mathrm{m}}/a$

If (4.12) is not satisfied, then the innermost mirror does not reach the centre of the CS (i.e. $k_{x,\mathrm{m}} x_{\mathrm{m}} \gg 1$). Instead, the mirrors closest to the centre with growth rate comparable to τ_{cs}^{-1} are most important, i.e. those located at $x_{\mathrm{m}} \sim \theta a$ (see (2.2)). Then the scaling laws in the previous section are modified; equations (4.13)–(4.17) become, respectively,

$$\gamma_{\mathrm{t,m}}^{\mathrm{FKR}} \tau_{\mathrm{A,r}} \sim \left(\frac{m_e}{m_i}\right)^{1/2} \left(\frac{d_i}{\theta a}\right)^{2}, \tag{4.18}$$

$$\frac{a(t_{\mathrm{cr}}^{\mathrm{FKR}})}{a_0} \lesssim \left(\frac{m_e}{m_i}\right)^{1/6} \left(\frac{d_i}{\theta a_0}\right)^{2/3} M_{\mathrm{A,0}}^{-1/3}, \tag{4.19}$$

$$\frac{a(t_{\mathrm{tr}})}{a_0} \lesssim \left(\frac{m_e}{m_i}\right)^{1/2} \left(\frac{d_i}{\theta a_0}\right), \tag{4.20}$$

$$\gamma_{\mathrm{t,m}}^{\mathrm{Coppi}} \tau_{\mathrm{A,r}} \sim \left(\frac{m_e}{m_i}\right)^{1/5} \left(\frac{d_i}{\theta a_0}\right), \tag{4.21}$$

$$\frac{a(t_{\mathrm{cr}}^{\mathrm{Coppi}})}{a_0} \lesssim \left(\frac{m_e}{m_i}\right)^{1/10} \left(\frac{d_i}{\theta a_0}\right)^{1/2}. \tag{4.22}$$

Comparing (4.19) and (4.20), we see that, if $d_i/(\theta a_0) \lesssim (m_e/m_i)^{-1} M_{\mathrm{A,0}}^{-1}$, tearing will onset before the fastest-growing mode can enter the large-Δ' regime (i.e. $t_{\mathrm{cr}}^{\mathrm{FKR}} < t_{\mathrm{tr}}$). In this case, a_{cr} is given by (4.19), which is larger by a factor of $\sim \theta^{-2/3}$ than a_{cr} derived without consideration of the mirrors, equation (3.2). Therefore, tearing will onset much sooner if $\theta \ll 1$, whereas t_{cr} is largely unaffected when $\theta \sim 1$. If, instead, $t_{\mathrm{cr}}^{\mathrm{FKR}} > t_{\mathrm{tr}}$, the mirror-stimulated tearing is Coppi-like, and a_{cr} is given by (4.22). However, the condition (4.12) still must be satisfied, allowing only a narrow range of validity for θ. Moreover, this range only exists if $d_i/a_0 \gg (m_e/m_i)^{-7/4} \beta_{\mathrm{r}}^{1/2} M_{\mathrm{A,0}}^{-2}$, a constraint not likely to be satisfied in the regime of interest. We therefore choose (4.19) as the relevant condition for the onset of mirror-stimulated tearing for $\theta \sim x_{\mathrm{m}}/a$.

5. Discussion

While the specific quantitative model of CS evolution and mirror-stimulated tearing formulated herein is perhaps debatable, it nevertheless demonstrates an important,

qualitative point: a gradually forming CS in a high-β, collisionless plasma easily produces enough pressure anisotropy to trigger the mirror instability, and the effect of this instability on the magnetic-field-line topology, and thus the tearing modes that instigate CS disruption via reconnection, ought to be considered.[6] For reasonable parameters, our theory predicts that the onset of reconnection in an evolving CS, driven by mirror-stimulated tearing modes, likely occurs earlier and at smaller scales than it would have without the mirrors, thereby placing a tighter upper limit on the aspect ratio of any forming CS (e.g. compare (4.14), (4.17) and (4.19) for the critical CS thickness at which mirror-stimulated tearing onsets to their $\Delta_p = 0$ counterpart, equation (3.2)). Whether or not these mirror-stimulated tearing modes ultimately grow to amplitudes $w \sim a_{\mathrm{eff}}$, and perhaps beyond to $\sim a$ via island coalescence, to disrupt the CS awaits further work.

An immediate practical implication of this result is that numerical simulations of collisionless reconnection in high-β plasmas should not initialize with a Maxwellian plasma embedded in an equilibrium CS. Instead, the CS should be allowed to evolve, and the particle distribution function self-consistently with it. A natural testing ground for this theory is the kinetic magnetorotational instability (MRI) (Quataert, Dorland & Hammett 2002; Heinemann & Quataert 2014), thought to be the main driver of turbulence and enhanced transport in collisionless accretion flows, such as that onto the supermassive black hole at the Galactic centre (Sharma *et al.* 2006). Historically, the linear MRI, at least in its MHD guise (Balbus & Hawley 1991), was quickly shown to be a nonlinear 'channel' solution in a differentially rotating disk (Goodman & Xu 1994), and various studies followed that employed Kelvin–Helmholtz and tearing 'parasitic' modes to disrupt the otherwise resilient channels. In some theories, this disruption is credited for setting the steady-state level of magnetorotational turbulence as a function of the dissipative properties of the underlying magnetized fluid (e.g. Pessah & Goodman 2009). Given that the kinetic MRI both linearly and nonlinearly drives pressure anisotropy (Squire, Quataert & Kunz 2017), it is worthwhile to contemplate a similar sequence of events, in which the kinetic MRI breaks down due to tearing modes stimulated by ion-Larmor-scale mirrors. Kinetic simulations of the MRI (e.g. Riquelme *et al.* 2012; Hoshino 2013, 2015; Kunz, Stone & Quataert 2016; Inchingolo *et al.* 2018) may already be capable of testing this idea.

Acknowledgements

REFERENCES

AMBROSIANO, J., LEE, L. C. & FU, Z. F. 1986 Simulation of the collisionless tearing instability in an anisotropic neutral sheet. *J. Geophys. Res.* **91**, 113–120.

ARCIS, N., LOUREIRO, N. F. & MILITELLO, F. 2009 Influence of higher-order harmonics on the saturation of the tearing mode. *Plasma Phys. Control. Fusion* **51** (3), 035002.

[6]In this respect, it is worth re-documenting the following prescient quote from the scarcely cited Coppi (1983): 'Thus we may consider the anisotropy-driven modes as a precursor of the spontaneous [tearing] ones and regard their effect as that of creating a region of macroscopic magnetic field turbulence near the neutral plane'.

BALBUS, S. A. & HAWLEY, J. F. 1991 A powerful local shear instability in weakly magnetized disks. I – Linear analysis. II – Nonlinear evolution. *Astrophys. J.* **376**, 214–233.

BARNES, A. 1966 Collisionless damping of hydromagnetic waves. *Phys. Fluids* **9**, 1483–1495.

BHATTACHARJEE, A., HUANG, Y.-M., YANG, H. & ROGERS, B. 2009 Fast reconnection in high-Lundquist-number plasmas due to the plasmoid instability. *Phys. Plasmas* **16** (11), 112102.

BOLDYREV, S. & LOUREIRO, N. F. 2017 Magnetohydrodynamic turbulence mediated by reconnection. *Astrophys. J.* **844**, 125.

BONAFEDE, A., FERETTI, L., MURGIA, M., GOVONI, F., GIOVANNINI, G., DALLACASA, D., DOLAG, K. & TAYLOR, G. B. 2010 The Coma cluster magnetic field from Faraday rotation measures. *Astron. Astrophys.* **513**, A30.

BRAGINSKII, S. I. 1965 Transport processes in a plasma. *Rev. Plasma Phys.* **1**, 205.

CARILLI, C. L. & TAYLOR, G. B. 2002 Cluster magnetic fields. *Annu. Rev. Astron. Astrophys.* **40**, 319–348.

CASSAK, P. A., BAYLOR, R. N., FERMO, R. L., BEIDLER, M. T., SHAY, M. A., SWISDAK, M., DRAKE, J. F. & KARIMABADI, H. 2015 Fast magnetic reconnection due to anisotropic electron pressure. *Phys. Plasmas* **22** (2), 020705.

CHAPMAN, S. & KENDALL, P. C. 1963 Liquid instability and energy transformation near a magnetic neutral line: a soluble non-linear hydromagnetic problem. *Proc. Phys. Soc. Lond.* A **271**, 435–448.

CHEN, J. & DAVIDSON, R. C. 1981 Tearing-mode stability properties of a diffuse anisotropic field-reversed ion layer at marginal stability. *Phys. Fluids* **24**, 2208–2215.

CHEN, J. & LEE, Y. C. 1985 Collsionless tearing instability in a non-Maxwellian neutral sheet – an integro-differential formulation. *Phys. Fluids* **28**, 2137–2146.

CHEN, J. & PALMADESSO, P. 1984 Tearing instability in an anisotropic neutral sheet. *Phys. Fluids* **27**, 1198–1206.

CHEW, G. F., GOLDBERGER, M. L. & LOW, F. E. 1956 The Boltzmann equation and the one-fluid hydromagnetic equations in the absence of particle collisions. *Proc. R. Soc. Lond.* A **236**, 112–118.

COMISSO, L., LINGAM, M., HUANG, Y.-M. & BHATTACHARJEE, A. 2017 Plasmoid instability in forming current sheets. *Astrophys. J.* **850**, 142.

COPPI, B. 1983 Magnetic reconnection driven by velocity space instabilities. *Astrophys. J. Lett.* **273**, L101–L106.

COPPI, B., GALVÃO, R., PELLAT, R., ROSENBLUTH, M. N. & RUTHERFORD, P. H. 1976 Fiz. Plazmy 2 (1976). *Sov. J. Plasma Phys.* **2** (533), 19.

DOBROWOLNY, M. 1968 Instability of a neutral sheet. *Nuovo Cimento B* **55**, 427–442.

DRAKE, J. F. & LEE, Y. C. 1977a Kinetic theory of tearing instabilities. *Phys. Fluids* **20** (8), 1341–1353.

DRAKE, J. F. & LEE, Y. C. 1977b Nonlinear evolution of collisionless and semicollisional tearing modes. *Phys. Rev. Lett.* **39**, 453–456.

DRAKE, J. F., SWISDAK, M., CHE, H. & SHAY, M. A. 2006 Electron acceleration from contracting magnetic islands during reconnection. *Nature* **443**, 553–556.

EGEDAL, J., LE, A. & DAUGHTON, W. 2013 A review of pressure anisotropy caused by electron trapping in collisionless plasma, and its implications for magnetic reconnection. *Phys. Plasmas* **20** (6), 061201.

ENßLIN, T. A. & VOGT, C. 2006 Magnetic turbulence in cool cores of galaxy clusters. *Astron. Astrophys.* **453**, 447–458.

FITZPATRICK, R. & PORCELLI, F. 2004 Collisionless magnetic reconnection with arbitrary guide field. *Phys. Plasmas* **11** (10), 4713–4718.

FITZPATRICK, R. & PORCELLI, F. 2007 Erratum: collisionless magnetic reconnection with arbitrary guide-field [2004 *Phys. Plasmas* **11**, 4713]. *Phys. Plasmas* **14** (4), 049902.

FURTH, H. P., KILLEEN, J. & ROSENBLUTH, M. N. 1963 Finiteresistivity instabilities of a sheet pinch. *Phys. Fluids* **6** (4), 459–484.

GINGELL, P. W., BURGESS, D. & MATTEINI, L. 2015 The three-dimensional evolution of ion-scale current sheets: tearing and drift-kink instabilities in the presence of proton temperature anisotropy. *Astrophys. J.* **802**, 4.

GOODMAN, J. & XU, G. 1994 Parasitic instabilities in magnetized, differentially rotating disks. *Astrophys. J.* **432**, 213–223.

GOVONI, F., MURGIA, M., VACCA, V., LOI, F., GIRARDI, M., GASTALDELLO, F., GIOVANNINI, G., FERETTI, L., PALADINO, R., CARRETTI, E. *et al.* 2017 Sardinia Radio Telescope observations of Abell 194. The intra-cluster magnetic field power spectrum. *Astron. Astrophys.* **603**, A122.

GUIDETTI, D., MURGIA, M., GOVONI, F., PARMA, P., GREGORINI, L., DE RUITER, H. R., CAMERON, R. A. & FANTI, R. 2008 The intracluster magnetic field power spectrum in Abell 2382. *Astron. Astrophys.* **483**, 699–713.

HAIJIMA, K., TANAKA, K. G., FUJIMOTO, M. & SHINOHARA, I. 2008 Electron temperature anisotropy effects on tearing mode in ion-scale current sheets. *Adv. Space Res.* **41**, 1643–1648.

HASEGAWA, A. 1969 Drift mirror instability of the magnetosphere. *Phys. Fluids* **12**, 2642–2650.

HEINEMANN, T. & QUATAERT, E. 2014 Linear Vlasov theory in the shearing sheet approximation with application to the magneto-rotational instability. *Astrophys. J.* **792**, 70.

HELLINGER, P. 2007 Comment on the linear mirror instability near the threshold. *Phys. Plasmas* **14**, 082105.

HOSHINO, M. 2013 Particle acceleration during magnetorotational instability in a collisionless accretion disk. *Astrophys. J.* **773**, 118.

HOSHINO, M. 2015 Angular momentum transport and particle acceleration during magnetorotational instability in a kinetic accretion disk. *Phys. Rev. Lett.* **114** (6), 061101.

HUANG, Y.-M., COMISSO, L. & BHATTACHARJEE, A. 2017 Plasmoid instability in evolving current sheets and onset of fast reconnection. *Astrophys. J.* **849**, 75.

INCHINGOLO, G., GRISMAYER, T., LOUREIRO, N. F., FONSECA, R. A. & SILVA, L. O. 2018 Fully kinetic large-scale simulations of the collisionless magnetorotational instability. *Astrophys. J.* **859**, 149.

KARIMABADI, H., DAUGHTON, W. & QUEST, K. B. 2005 Physics of saturation of collisionless tearing mode as a function of guide field. *J. Geophys. Res. (Space Physics)* **110**, A03214.

KUNZ, M. W., SCHEKOCHIHIN, A. A. & STONE, J. M. 2014 Firehose and mirror instabilities in a collisionless shearing plasma. *Phys. Rev. Lett.* **112** (20), 205003.

KUNZ, M. W., STONE, J. M. & QUATAERT, E. 2016 Magnetorotational turbulence and dynamo in a collisionless plasma. *Phys. Rev. Lett.* **117** (23), 235101.

LE, A., DAUGHTON, W., KARIMABADI, H. & EGEDAL, J. 2016 Hybrid simulations of magnetic reconnection with kinetic ions and fluid electron pressure anisotropy. *Phys. Plasmas* **23** (3), 032114.

LE, A., EGEDAL, J., DAUGHTON, W., FOX, W. & KATZ, N. 2009 Equations of state for collisionless guide-field reconnection. *Phys. Rev. Lett.* **102** (8), 085001.

LOUREIRO, N. F. & BOLDYREV, S. 2017*a* Collisionless reconnection in magnetohydrodynamic and kinetic turbulence. *Astrophys. J.* **850**, 182.

LOUREIRO, N. F. & BOLDYREV, S. 2017*b* Role of magnetic reconnection in magnetohydrodynamic turbulence. *Phys. Rev. Lett.* **118** (24), 245101.

LOUREIRO, N. F., COWLEY, S. C., DORLAND, W. D., HAINES, M. G. & SCHEKOCHIHIN, A. A. 2005 X-Point collapse and saturation in the nonlinear tearing mode reconnection. *Phys. Rev. Lett.* **95** (23), 235003.

LOUREIRO, N. F., SCHEKOCHIHIN, A. A. & COWLEY, S. C. 2007 Instability of current sheets and formation of plasmoid chains. *Phys. Plasmas* **14** (10), 100703.

LOUREIRO, N. F. & UZDENSKY, D. A. 2016 Magnetic reconnection: from the Sweet–Parker model to stochastic plasmoid chains. *Plasma Phys. Control. Fusion* **58** (1), 014021.

MALLET, A., SCHEKOCHIHIN, A. A. & CHANDRAN, B. D. G. 2017*a* Disruption of Alfvénic turbulence by magnetic reconnection in a collisionless plasma. *J. Plasma Phys.* **83** (6), 905830609.

MALLET, A., SCHEKOCHIHIN, A. A. & CHANDRAN, B. D. G. 2017*b* Disruption of sheet-like structures in Alfvénic turbulence by magnetic reconnection. *Mon. Not. R. Astron. Soc.* **468**, 4862–4871.

MARRONE, D. P., MORAN, J. M., ZHAO, J.-H. & RAO, R. 2007 An unambiguous detection of Faraday rotation in sagittarius A*. *Astrophys. J. Lett.* **654**, L57–L60.

MATTEINI, L., LANDI, S., VELLI, M. & MATTHAEUS, W. H. 2013 Proton temperature anisotropy and magnetic reconnection in the solar wind: effects of kinetic instabilities on current sheet stability. *Astrophys. J.* **763**, 142.

PARKER, E. N. 1957 Sweet's mechanism for merging magnetic fields in conducting fluids. *J. Geophys. Res.* **62**, 509–520.

PESSAH, M. E. & GOODMAN, J. 2009 On the saturation of the magnetorotational instability via parasitic modes. *Astrophys. J. Lett.* **698**, L72–L76.

PUCCI, F. & VELLI, M. 2014 Reconnection of quasi-singular current sheets: the 'ideal' tearing mode. *Astrophys. J. Lett.* **780**, L19.

QUATAERT, E. 2003 Radiatively inefficient accretion flow models of Sgr A*. *Astron. Nachr. Suppl.* **324**, 435–443.

QUATAERT, E., DORLAND, W. & HAMMETT, G. W. 2002 The magnetorotational instability in a collisionless plasma. *Astrophys. J.* **577**, 524–533.

QUEST, K. B., KARIMABADI, H. & DAUGHTON, W. 2010 Linear theory of anisotropy driven modes in a Harris neutral sheet. *Phys. Plasmas* **17** (2), 022107.

RINCON, F., SCHEKOCHIHIN, A. A. & COWLEY, S. C. 2015 Non-linear mirror instability. *Mon. Not. R. Astron. Soc.* **447**, L45.

RIQUELME, M. A., QUATAERT, E., SHARMA, P. & SPITKOVSKY, A. 2012 Local two-dimensional particle-in-cell simulations of the collisionless magnetorotational instability. *Astrophys. J.* **755**, 50.

RIQUELME, M. A., QUATAERT, E. & VERSCHAREN, D. 2015 Particle-in-cell simulations of continuously driven mirror and ion cyclotron instabilities in high beta astrophysical and heliospheric plasmas. *Astrophys. J.* **800**, 27.

RUTHERFORD, P. H. 1973 Nonlinear growth of the tearing mode. *Phys. Fluids* **16**, 1903–1908.

SCHEKOCHIHIN, A. A. & COWLEY, S. C. 2006 Turbulence, magnetic fields, and plasma physics in clusters of galaxies. *Phys. Plasmas* **13** (5), 056501.

SCHEKOCHIHIN, A. A., COWLEY, S. C., KULSRUD, R. M., ROSIN, M. S. & HEINEMANN, T. 2008 Nonlinear growth of firehose and mirror fluctuations in astrophysical plasmas. *Phys. Rev. Lett.* **100** (8), 081301.

SCHOEFFLER, K. M., DRAKE, J. F. & SWISDAK, M. 2011 The effects of plasma beta and anisotropy instabilities on the dynamics of reconnecting magnetic fields in the heliosheath. *Astrophys. J.* **743**, 70.

SHARMA, P., HAMMETT, G. W., QUATAERT, E. & STONE, J. M. 2006 Shearing box simulations of the MRI in a collisionless plasma. *Astrophys. J.* **637**, 952–967.

SHI, Y., LEE, L. C. & FU, Z. F. 1987 A study of tearing instability in the presence of a pressure anisotropy. *J. Geophys. Res.* **92**, 12171–12179.

SOUTHWOOD, D. J. & KIVELSON, M. G. 1993 Mirror instability. I – Physical mechanism of linear instability. *J. Geophys. Res.* **98**, 9181–9187.

SQUIRE, J., QUATAERT, E. & KUNZ, M. W. 2017 Pressure-anisotropy-induced nonlinearities in the kinetic magnetorotational instability. *J. Plasma Phys.* **83** (6), 905830613.

SWEET, P. A. 1958 The neutral point theory of solar flares. In *Electromagnetic Phenomena in Cosmical Physics* (ed. B. Lehnert), IAU Symposium, vol. 6, p. 123. Cambridge University Press.

TENERANI, A., VELLI, M., RAPPAZZO, A. F. & PUCCI, F. 2015 Magnetic reconnection: recursive current sheet collapse triggered by ideal tearing. *Astrophys. J. Lett.* **813**, L32.

TOLMAN, E. A., LOUREIRO, N. F. & UZDENSKY, D. A. 2018 Development of tearing instability in a current sheet forming by sheared incompressible flow. *J. Plasma Phys.* **84** (1), 905840115.

UZDENSKY, D. A. & LOUREIRO, N. F. 2016 Magnetic reconnection onset via disruption of a forming current sheet by the tearing instability. *Phys. Rev. Lett.* **116** (10), 105003.

VACCA, V., MURGIA, M., GOVONI, F., FERETTI, L., GIOVANNINI, G., PERLEY, R. A. & TAYLOR, G. B. 2012 The intracluster magnetic field power spectrum in A2199. *Astron. Astrophys.* **540**, A38.

WAELBROECK, F. L. 1989 Current sheets and nonlinear growth of the m=1 kink-tearing mode. *Phys. Fluids* B **1**, 2372–2380.

WAELBROECK, F. L. 1993 Onset of the sawtooth crash. *Phys. Rev. Lett.* **70**, 3259–3262.

YAMADA, M., KULSRUD, R. & JI, H. 2010 Magnetic reconnection. *Rev. Mod. Phys.* **82**, 603–664.

ZWEIBEL, E. G. & YAMADA, M. 2009 Magnetic reconnection in astrophysical and laboratory plasmas. *Annu. Rev. Astron. Astrophys.* **47**, 291–332.